Domain-growth kinetics for the Q-state Potts model in two and three dimensions

Gary S. Grest and Michael P. Anderson
Corporate Research Science Laboratory, Exxon Research and Engineering Company, Clinton Township, Route 22 East, Annandale, New Jersey 08801

David J. Srolovitz
Department of Materials Science and Engineering, University of Michigan, Ann Arbor, Michigan 48109
(Received 21 December 1987)

We present new simulations of the domain-growth kinetics for the Q-state Potts model in two and three dimensions. The time dependence of the average grain radius $\bar{R}$ can be described by $\bar{R} \cong Bt^n$, where B is a temperature-dependent constant. In two dimensions, we find $n = 0.49 \pm 0.02$ for a range of Q values from 2 to 48. This value of n is obtained from very long simulations on lattices up to size 1000^2 and is in contrast to our earlier estimates for n which were less than $\frac{1}{2}$ ($n \cong 0.41 \pm 0.01$) for large Q. In three dimensions on lattices of size 100^3, we find that $n = 0.48 \pm 0.04$ if early-time data are excluded from the fit to the kinetic data but smaller if the entire data set is used. The grain-size distribution for several values of Q in both two and three dimensions is also determined and compared with our results for grain growth in real polycrystalline materials.

I. INTRODUCTION

During the past few years, there has been a considerable effort[1-17] to understand the kinetics of domain growth in systems with a high ground-state degeneracy which have been quenched from a high-temperature disordered state, $T \gg T_c$, to a final temperature below the transition temperature T_c. After the quench the system spontaneously develops local domains which are highly ordered. The average domain size grows in order to reduce the excess free energy associated with the domain walls. For the nonconserved Ising model,[18] which has a ground-state degeneracy of 2, it has been known since the work of Lifshitz[1] and Allen and Cahn[19] that the correlation length R grows algebraically as $t^{1/2}$ for all dimensions above one. This result has been well documented by both analytical[18-26] and computer simulation studies[18,21,24-26] as well as experiments on ordered alloys[19] (e.g., Fe-Al and Cu-Au). However, until about five years ago little was known about the growth kinetics for more complex models which have a higher ground-state degeneracy. Lifshitz[1] was the first to predict slow kinetics in systems with several degenerate equilibrium states. Safran[2] extended these arguments to show that domains may become pinned if the number of degenerate ground states $Q \geq d+1$, where d is the dimension of space. They suggested that the system could become trapped in local metastable states which would then greatly slow down the kinetics. Following these ideas, we[3-5] carried out computer simulations to study the kinetics of the two-dimensional Q-state ferromagnetic Potts model, for a wide range of Q's from the $Q=2$ Ising model to $Q=64$. While we[3-5] found that the growth remained algebraic, independent of the value of Q, we also found that the higher ground-state degeneracy had an effect on the growth kinetics, the microstructure, and the topology.

In general, the time dependence of the average grain radius $\bar{R}$ can be described by

$$\bar{R} \cong Bt^n , \tag{1}$$

where B is a temperature-dependent constant. For the Ising model, it is well known[18-26] that $n = \frac{1}{2}$. In our early studies,[3-5] we observed that the exponent n for growth in the two-dimensional (2D) Potts model was dependent on Q. As Q increased from 2, n decreased slowly from 0.5 to approximately 0.41 ± 0.02 for Q greater than approximately 30. As Q increased the grains became more compact and the domain size distribution function narrowed. For Q larger than approximately 30, we found both n and the domain size distribution function become independent of Q. This result for large Q was confirmed independently by Wejchert *et al.*[15] and Mouritsen.[16] However, as pointed out by a number of authors,[9,12,27,28] it is difficult to determine whether the exponents one obtains from fitting the simulation results are truly asymptotic. This is true even when the available data give an excellent fit to Eq. (1). It is always difficult to rule out slow transients. Our original simulations[3-5] were carried out on lattices of size 200×200, which were already much larger than those used to study equilibrium critical phenomena. Such large lattices were necessary since we were interested in following the kinetics for long times. However, even for this size system, we had to stop the simulation when the average grain size was of order 200 sites, in order to ensure that there were enough domains in the system to give representative results and avoid the influence of boundary conditions. Because the average area grows as $\bar{R}^2 \simeq t^{2n}$, very large systems are needed to extend the time regime significantly. In this paper we report new results on lattices as large as 1000×1000 that show, in fact, when the simulations are extended to much larger systems and longer times the value of n for all Q studied in-

 ©1988 The American Physical Society

creases to $n=0.49\pm0.02$, consistent with that for the Ising model. However, all of our other results for the domain size and topological distributions remain essentially unchanged.

In addition to the simulations on large lattices in 2D, we have extended our simulations to three dimensions (3D), where we have studied systems as large as 100^3. (Although the 2D 1000^2 lattices and the 3D 100^3 lattices contain the same number of sites, it is important to note that the maximum linear dimension of domains in the 2D samples is a factor of 10 larger than for the 3D study.) Here we observe values of n which are less than $\frac{1}{2}$ for large Q if data for times $t \geq 200$ Monte Carlo steps per spin are included. In this case, we[17] find that for Q larger than approximately 12, n is independent of Q and $n=0.39\pm0.02$. However, when more of the early time data are excluded, we find $n=0.48\pm0.04$ for large Q. We[17] also find that the microstructures and topological distribution function depend only very weakly on dimensionality. The distribution of grain areas from our 2D simulations are very similar to the cross sections from our 3D simulations. While the shape of the distribution functions change with Q, they are relatively insensitive to dimensionality. We also find that the grain size and topological distribution functions for the high-Q Potts model agree very well with grain growth microstructures of real polycrystalline materials.

In this paper we present new simulation results in 2D on systems of size 380^2 and 1000^2 and in 3D on systems of size 100^3 for $3 \leq Q \leq 48$. In Sec. II we briefly describe the model and the Monte Carlo procedure. Our results for the growth kinetics and domain size distributions are presented in Sec. III. We also compare our large Q results with experimental data for polycrystalline materials. Finally, in Sec. IV, we discuss some of the implications of these results.

II. MODEL AND METHOD

The Hamiltonian for the Q-component ferromagnetic Potts model with a nonconserved order parameter is given by

$$H=-J\sum\delta_{S_iS_j}\ , \tag{2}$$

where S_i is the state of the spin on site i ($1 \leq S_i \leq Q$) and δ_{ab} is the Kronecker δ function. The sum is over all spin pairs within a specified distance and J is a positive constant. For all of the simulations, we started the system in a random state and rapidly quenched to $T \simeq 0$. The kinetics of the boundary motion were simulated via a Monte Carlo method in which a site is selected at random and reorientated to a randomly chosen orientation. A generalization[3] of Bortz *et al.*[29] "n fold" or continuous time technique to the Potts model was employed to make the simulations more efficient. Without this method, the number of runs and size of the systems which we would have been able to study would have been greatly reduced. This is particularly true for large Q and late times, when most of the spins are not on the boundary. N reorientation attempts per site are referred to as one Monte Carlo step (MCS), where N is the number of lattice sites. Periodic boundary conditions were employed in all of the simulations.

In 2D, we have carried out simulations on triangular and square lattices with sizes ranging from 200^2 to 1000^2. For the triangle lattice, we include only nearest-neighbor (NN) interactions in Eq. (2). We[3] found that on the square lattice if only NN are included, the domains become pinned for quenches to $T \simeq 0$ and the growth exponent n is zero for $Q \geq 3$, in accord with the predictions of Lifshitz[1] and Safran.[2] When the range of interaction is extended beyond NN to include next nearest neighbors (NNN) with coupling J equal for NN and NNN pairs, domain walls are not pinned and $\bar{R}$ increases algebraically with the same value of n as on the triangle lattice.[3] Viñals and Gunton[13] found that if J is not exactly equal for the NN and NNN interactions, the domains become pinned for quenches to $T \simeq 0$. When the final quench temperature[3] $T>0$, the growth on the square lattice with NN interactions is not pinned and we observed an effective growth exponent n which was T dependent rising toward the values observed on the triangle lattice with increasing T. In 3D, similar effects occur for the simple cubic (sc) lattice for $Q>3$. When the sum is only taken over NN in Eq. (2), domain growth becomes pinned as there is no local driving force on the vertices where four domains meet. However, the introduction of further neighbors in the sum [Eq. (2)] unpins the system and growth occurs even for $T \simeq 0$. In 3D, we[17] have studied systems of size 60^3 and 100^3 on the simple cubic lattice, including 6, 18, 26, and 124 neighbors in the sum in Eq. (2). This corresponds to the inclusion of NN sites, NN plus NNN sites, all sites within a cube out to (111) and all sites within a cube out to (222), respectively. We refer to these as cases $k=1$, 2, 3, and 4. As the number of neighbors increases, the interaction becomes more spherical, eliminating effects due to the underlying lattice. We have only investigated the case in which the coupling J is equal for all pairs within the range of interaction. When the final quench temperature $T>0$, the domains in the sc lattice with only NN interactions do become unpinned, but the effective exponent n increases only slightly before T_c is reached. Since our main aim has been to search for universal features which describe the growth kinetics, we have concentrated on systems which do not become pinned due to local lattice effects[30] when quenched to $T \simeq 0$.

On the square lattice, all of the results presented are averaged over five runs on a 380^2 lattice. We will also present results for the $Q=48$ model on a 1000^2 triangle lattice averaged over two runs as well as data on a 200^2 lattice which were averaged over 15 runs, to make comparison with our earlier studies. In 3D, we will present results on a 100^3 sc lattice. For low Q, our results are averaged over two to three runs, while for large Q, we typically made only one run. This is for two reasons. The first was computer time: a single run for a $Q=48$ 100^3 simulation takes approximately 12–15 h of CPU time on an IBM 3090/150 computer with $k=3$. Since the continuous time method we use in the simulations is scalar in its design, the amount of CPU time decreases

only slightly on a Cray supercomputer. The second is that we see little fluctuation in our results from sample to sample. For high Q, there is a sufficient number of domains to obtain good statistics for both the domain size and topological distributions from one run. Two runs for $k=3$, $Q=48$ on the 100^3 lattice gave nearly identical results for all properties studied. However, for small Q, where the domains are less compact, the small linear dimension of our 3D simulations does begin to play a role, limiting the time we can follow the growth and increasing the magnitude of the statistical fluctuations. For the Potts model, unlike the Ising model, the growth kinetics can easily be monitored by measuring the average grain area or volume directly by using a cluster-enumeration routine. Both of these quantities are strongly self-averaging[14] unlike $\bar{L}(t)=L^d\langle\psi^2\rangle_t/\langle\psi^2\rangle_T$, which is not self-averaging,[31] where ψ is the order parameter and $\langle\ \rangle_t$ and $\langle\ \rangle_T$ denote the time-dependent and equilibrium averages, respectively. Measuring the average area or volume is computationally efficient and gives an accurate measure of the growth without having to average over many samples as is usually necessary for the Ising model. While it would be advantageous to use larger lattices in 3D to follow the growth for very long times, this is not possible with our present resources.

III. RESULTS

In Fig. 1 we display the microstructures for $Q=3$, 6, 12, and 48 simulations on the 2D square lattice with NN and NNN interactions. The boundary is drawn as the perpendicular bisector between misoriented NN sites. One can clearly see the gross morphogical changes that occur as Q increases from near the Ising value ($Q=2$) toward the limit of high Q. The low-Q configurations consist of very irregular and asymmetric domains. This irregularity decreases as Q increases. For high Q, the domains are significantly more compact and equiaxed. This dependence of the domain morphology on Q is very similar in 3D, as shown in Fig. 2 where we plot a (100) planar section through the sc lattice for $k=2$ (18 neighbors) and 3 (26 neighbors) for the same values of Q. In Refs. 14 and 17 we presented microstructures of the temporal evolution of the growth on the square lattice with

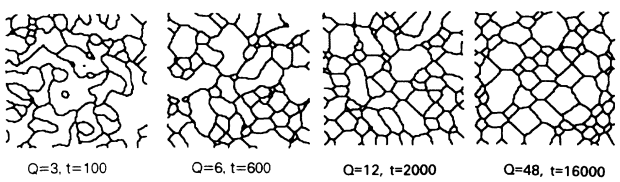

FIG. 1. Domain-boundary configurations for $Q=3$, 6, 12, and 48 Potts model on a square lattice that were quenched from $T\gg T_c$ to $T=0$. Solid curves represent the boundaries between the regions of different orientations. The times were chosen to yield comparable domain sizes. A 200^2 section of the 380^2 sample is shown.

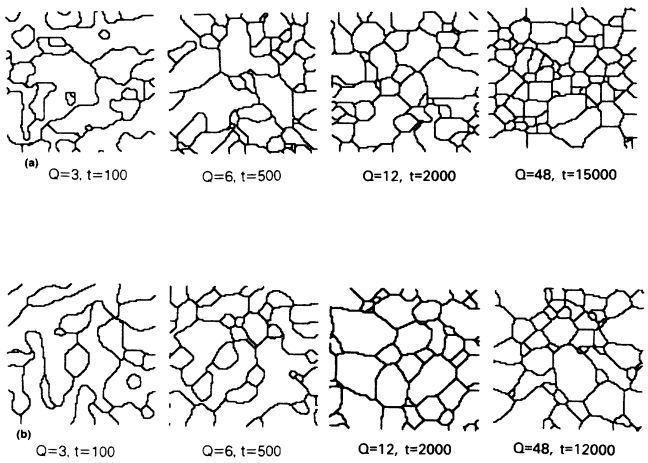

FIG. 2. Planar (100) cross section of the 3D microstructure for a 100^3 sc lattice with $Q=3$, 6, 12, and 48 for (a) $k=2$ and (b) $k=3$. The times were chosen to yield comparable domain sizes.

NN and NNN interactions and on the simple cubic lattice with interaction range $k=2$, 3, and 4 for a number of values for Q. The results for the square lattice are nearly identical to those on the triangle lattice presented in Ref. 3. From these microstructures, it is clear that in the low-Q limit, large discontinuous changes in the area of individual grains can occur when one domain meets and coalesces with another domain with the same orientation. The probability of such change meetings decreases as Q increases, though one can see occurrences of this in the micrographs for Q as large as 30. Since such coalescence events are strictly forbidden in the limit $Q\rightarrow\infty$, the rarity of such events for $Q\geq 36$ indicates that the infinitely degenerate system can be modeled with a large finite Q. An example of a highly degenerate system is the grain structure of polycrystalline materials, where the Q orientations can be associated with the Ising value ($Q=2$) toward the limit of high Q. Boundaries for the $k=2$ case are flatter; reminiscent of the 2D square lattice with NN interaction,[3] which becomes pinned by T shaped vertices where three domains meet. The longer range interaction in the $k=3$ case which has a more isotropic grain boundary energy seems to eliminate these, producing grain boundaries which on a coarser scale meet at 120° even though the sc lattice grain boundaries which meet at triple lines are constrained to meet at either 90° or 180°, due to the symmetry of the lattice.

The domain size distribution functions are shown in Fig. 3 for the 2D square lattice with NN and and NNN interactions and for that obtained from (100) planar cross sections through both the $k=2$ and 3 models on the sc lattice for $Q=6$, 12, and 48. Results for the triangular lattice with NN interactions are indistinguishable to those for the square lattice with equal strength NN and NNN interactions. For $Q\leq 4$, the 100^3 lattices are too small to obtain good statistics for the volume, V, or cross-sectional area, A, distributions but the linear inter-

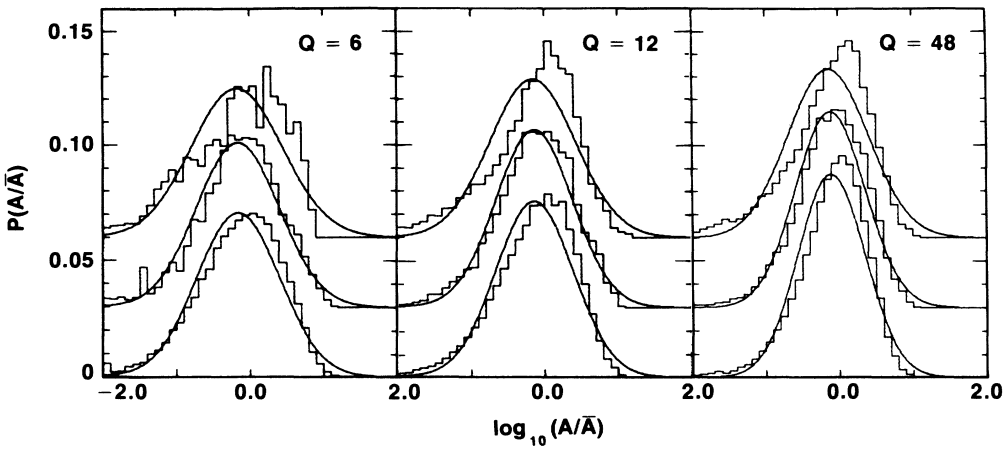

FIG. 3. Time-averaged domain size distribution function $f(\log_{10}A/\bar{A})$, for $Q=6$, 12, and 48 for the square lattice (bottom curve) and sc lattice with $k=2$ (middle curve) and $k=3$ (top curve). The upper two curves have been displaced vertically by 0.03 and 0.06, respectively, for clarity. The solid line corresponds to the log-normal function with appropriate values for the mean and standard deviation as determined from the histograms.

cept can be obtained. The 2D results are nearly identical with the $k=2$ sc results and both differ only slightly from the $k=3$ sc case. In cross section there appear to be more small grains for the $k=3$ sc case than for the other two cases. These distributions were found to be time invariant when normalized by their respective means. This property, which is referred to as statistical self-similarity, was always observed at late times. The only data available to test how well our model compares with experimental data is for polycrystalline materials. In Fig. 4, we present the linear grain-size distribution from our simulations for the $k=3$ model with $Q=48$ and data for pure Fe.[17(b)] Note that the grain-size distribution function for the simulations and experiment agree remarkably well.

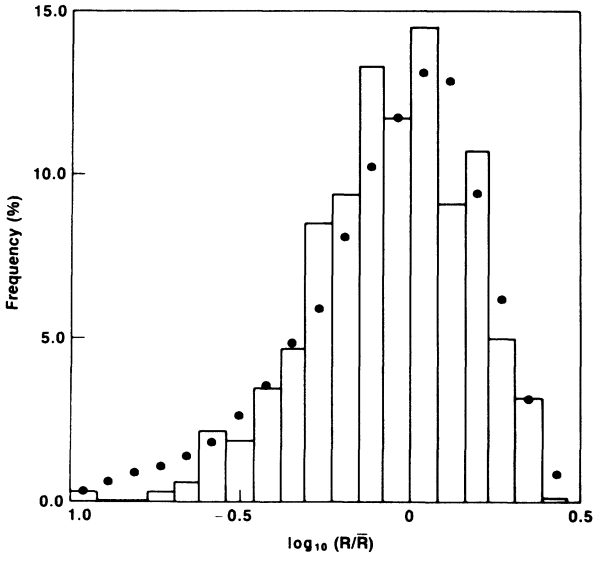

FIG. 4. Grain radius distribution as determined from a cross-sectional area analysis of pure Fe (histogram) and from cross sections of the three-dimensional $k=3$ lattice model (solid circles).

Also shown in Fig. 3 as the continuous curve is the log-normal function $f(\log_{10}x)$, where $x=A/\bar{A}$, plotted using the values for the mean μ and standard deviation σ measured for each distribution. Note that the log-normal function is symmetric on the logarithmic scale employed and has tails extending to $\pm\infty$ while the data is actually skewed. The log-normal form is a better representation of our data for small Q[5]. The development of the log-normal distribution in domain growth has been rationalized[32] in terms of a probabilistic mechanism in which individual domains are assumed to change area or volume in a random and uncorrelated manner. This argument is not appropriate for high Q, where the density of vertices is high. The presence of vertices couples each domain to its neighbors, so that changes in area or volume are correlated. In this limit, we find a better fit between the cross-sectional data and Louat's function:[33] $f(A/\bar{A})=\exp(-A/\bar{A})$. However, the volume distribution $f(\log_{10}(V/\bar{V}))$ is better fit by a log-normal function.[17(b)] In Ref. 17(b) we also present results for the relationship between the number of faces, corners, and edges for individual grains and the frequency of the number of grain faces as well as a more detailed analysis of the grain-size distribution functions for $Q=36$ and 48 in both two and three dimensions.

Domain-growth kinetics were evaluated by monitoring the time evolution of the mean chord length $\bar{L}$, mean cross-sectional area $\bar{A}$, and mean domain volume $\bar{V}$ (in 3D). Data for the time dependence of the area $\bar{A}$ are shown in Fig. 5 for four values of Q on the 2D square lattice with NN and NNN interactions. The lattice size is 380^2 and the data is presented as both a log-log and linear-linear plot. Data for the $k=2$ and 3 model in 3D on a 100^3 lattice are shown in Fig. 6. These data can be fit to the kinetic equation:

$$X(t)^m - X(0)^m = Bt \ , \tag{3}$$

where X is equal to either $\bar{L}$, $\bar{A}$, or $\bar{V}$. For $X(t) \gg X(0)$, Eq. (3) reduces to $\bar{R} = Bt^n$, Eq. (1), where $\bar{R} = \bar{X}^{1/d}$ and $n = 1/(md)$, where $d = 1$ for $\bar{L}$, 2 for $\bar{A}$, and 3 for $\bar{V}$. The average growth exponent n determined from fitting $\bar{L}$ or $\bar{A}$ in 2D or $\bar{L}$, $\bar{A}$, and $\bar{V}$ in 3D give the same result within statistical error. Results for growth in 2D indicate that $N = 0.49 \pm 0.02$ for all Q. As can be seen from Fig. 5(b), the late time results seem to be quite linear on the plot of $\bar{A}$ versus t. Our new results for $Q = 48$ on a 1000^2 triangle lattice out to 60 000 MCS (see Fig. 7), give $n = \frac{1}{2}$, in agreement with the result for the square lattice, and fall on top of the early time data ($t \leq 6000$) on the 200^2 lattice. Both of these results give a value of n which is greater than our previous estimates of 0.41 ± 0.02 for $Q \geq 30$. As seen from Fig. 5(a), there is significant curvature in the early time regime for high Q and this is apparently the reason we obtained a lower estimate of n for

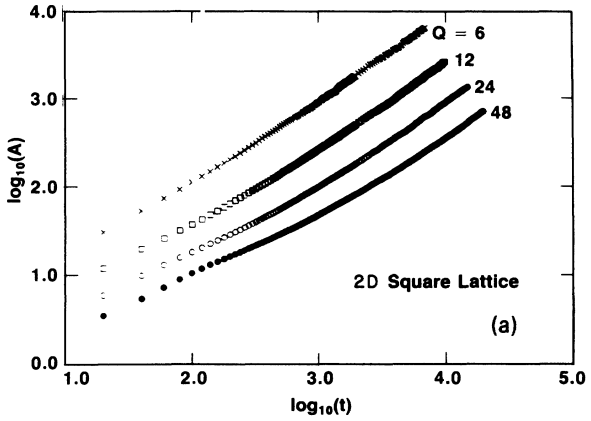

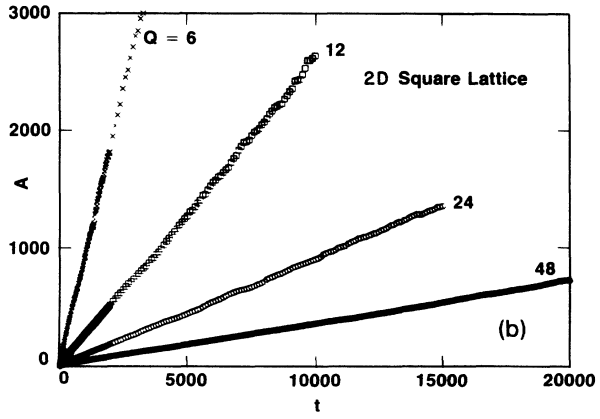

FIG. 5. Plot of average area $\bar{A}$ vs t(MCS) for the $Q = 6$, 12, 24, and 48 Potts model following a quench from $T \gg T_c$ to $T = 0$. Data is averaged over five runs on a 380^2 square lattice with NN and NNN interactions of equal strength. In (a) we show the data on a log-log and (b) on a linear-linear plot. The exponent n is obtained by least-square fitting this data to Eq. (3).

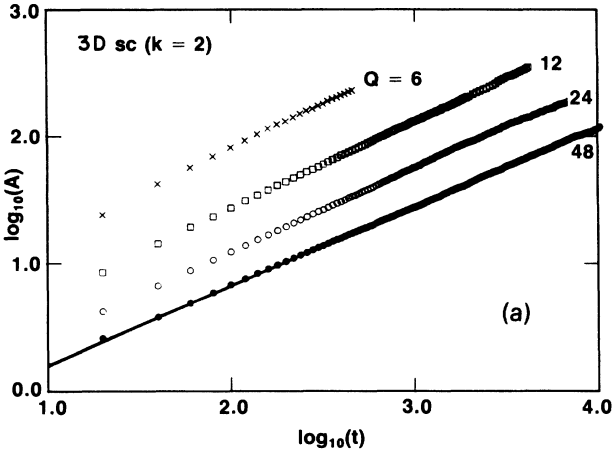

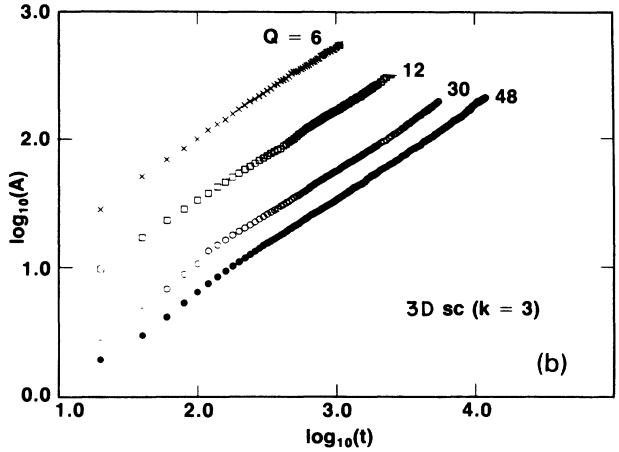

FIG. 6. Plot of $\log_{10}(\bar{A})$ vs $\log_{10}(t)$ for the Potts model on a 100^3 sc lattice for four values of Q for (a) $k = 2$ and (b) $k = 3$.

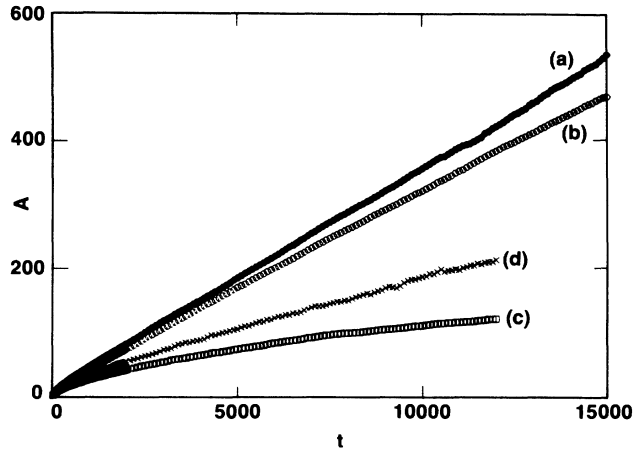

FIG. 7. Average area $\bar{A}$ vs t on a linear scale for $Q = 48$ Potts model on (a) 380^2 square lattice with NN and NNN interactions, (b) 1000^2 triangle lattice with NN interactions, (c) 100^3 sc lattice with $k = 2$ and (d) 100^3 sc lattice with $k = 3$.

high Q from fitting Eq. (3) to our original data.[3,4] If we fit our new data for $t \leq 4000$ MCS, we obtain estimates for n which are consistent with our previous results, indicating the rather slow crossover to the asymptotic time regime and the need to do long simulations which require large lattices.

In fitting the available simulation data in 3D to determine the kinetic exponent, we found that the results were sensitive to the time regime examined. When all data for time $t \geq 200$ MCS was included in the least-square fit to Eq. (3), the grain growth exponent obtained for $Q \geq 12$ is approximately[17(b)] $n = 0.28 \pm 0.02$ for $k = 2$ and $n = 0.39 \pm 0.02$ for $k = 3$ and 4. These were the exponents we reported in an earlier short communication[17(a)] and an earlier review on the 3D work.[14] However, we now know from our work for 2D, as discussed above, that inclusion of short time data results in artificially low exponents. To rigorously check this possibility for the 3D kinetic data, it is desirable to run this simulation to longer times as we did in 2D. Unfortunately, the maximum lattice size which can currently be treated is 100^3, and the data have been collected to the time and grain-size limits imposed by this lattice size. Therefore, the only recourse at this time is to carefully examine the data for a possible crossover from short time $n = 0.39$ kinetics to kinetics with larger n. Figure 7 shows a plot of the cross-

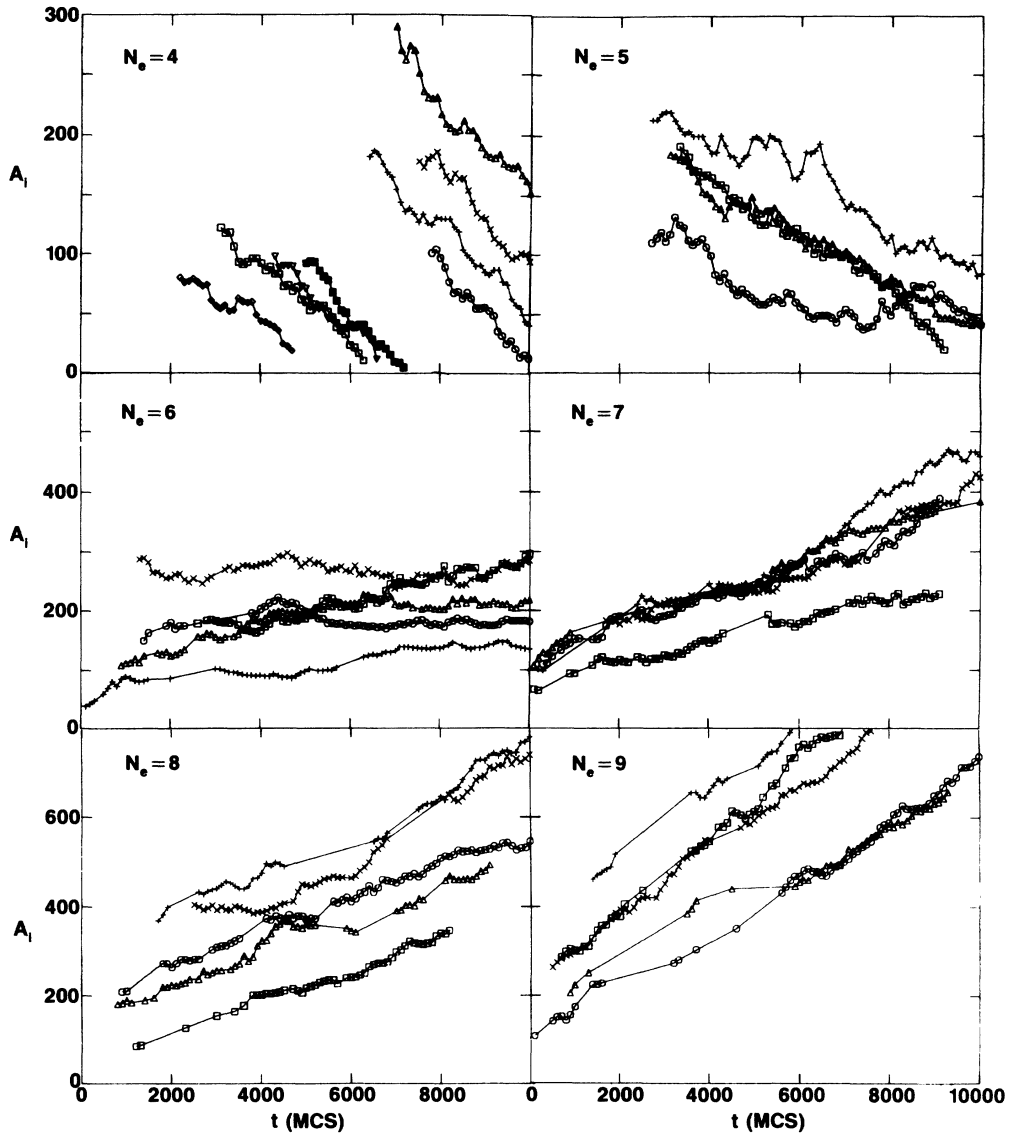

FIG. 8. Time dependence of the area A_i of individual grains from the 2D simulation with a specific number of edges N_e on the triangle lattice. Symbols are shown every 20 MCS when the grain has the number of edges specified. The simulations were started from a random starting state and run for 1000 MCS, after which the clock was reset to 0. The data plotted are for grains which had the specified number of edges over unusually large portions of the next 10 000 MCS.

sectional area versus time for $Q=48$ for $k=2$ and 3. The $k=2$ data do not exhibit a linear regime for the time scale studied, indicating that if a crossover to $n=0.5$ occurs, it does so for times much longer than those currently examined. The $k=3$ data have a curved region at small time, followed by a linear behavior at large time. Fits to these long time data ($t \geq 2000-4000$ MCS for $k=3$ and $t \geq 1000$ MCS for $k=4$) presented in Ref. 17(b), yield a kinetic exponent of $n=0.48\pm0.04$. The numerical fitting parameters obtained from least-square fitting to Eq. (3) are tabulated in Table I of Ref. 17(b) for $Q=30$ and 48. The $k=3$ and 4 data obey Eq. (3) with $n=0.48$ at large time, but not for short time.

The long-time linearity of the $\bar{A}$ versus t plots (Fig. 7) and our experience with small and large lattices in 2D together strongly suggest that the asymptotic growth kinetics are of the form $\bar{R}=Ct^{0.5}$. The apparently lower exponents found when short-time data are also included are presumably due to the presence of two competing length scales in the simulation: namely, the mean grain size and the lattice spacing, a_0 as suggested by Kumar *et al.*[9] and Beenakker.[34] The effect of the finite lattice spacing is reduced as $\bar{R}$ grows but is only completely negligible in the limit $\bar{R} \gg a_0$. Only in this limit can we expect the growth to be strictly self-similar. Nevertheless, the grain size and topological distributions presented above do appear to be evolving in a self-similar manner.

IV. DISCUSSION

One interesting problem which requires more attention is why the growth exponent n appeared to be less than $\frac{1}{2}$ for high Q in our earlier 2D simulations and for both the simulations and experiment in 3D. In 2D, Mullins[35] has shown that only by assuming statistical self-similarity (which our simulations appear to demonstrate) and local equilibrium that n must equal $\frac{1}{2}$. He uses the result, first proven by von Neumann[36] and Mullins,[37] that for both bubble growth and idealized grain growth in 2D, the rate of change of the area A_i of an individual grain (or bubble) depends only on the number of sides,

$$A \equiv \frac{dA_i}{dt} = \frac{\pi k}{3}(N_e - 6) , \tag{4}$$

where k is constant. This equation should be valid for an arbitrarily shaped 2D grain of N_e sides under the assumption that the local velocity $u=k/R$ and the angle between the intersecting grain boundaries is 120°. (R is the signed local radius of curvature lying in the plane, counted positive when it lies along the normal.) Thus $A_i>0$ for $N_e>6$ and is <0 for $N_e<6$. The statistical self-similarity hypothesis may be written in the form

$$f_{N_e}(A,t)=\phi(A/\bar{A})/\bar{A} , \tag{5}$$

where $f_N(A,t)$ is the probability that a grain has N_e edges and area A between A and $A+dA$. Mullins[35] then proves that if local equilibrium is satisfied [i.e., Eq. (4) is valid for all grains at all times] then $n=\frac{1}{2}$.

Since we have already shown that Eq. (5) is valid,[5,17(b)] it is of interest to examine Eq. (4) more closely in order to understand the apparent slow crossover to asymptotic behavior. This is particularly interesting in light of the simulations by Wejchert *et al.*[15] for 2D soap bubbles, who using a procedure similar to ours, introduced the ad-

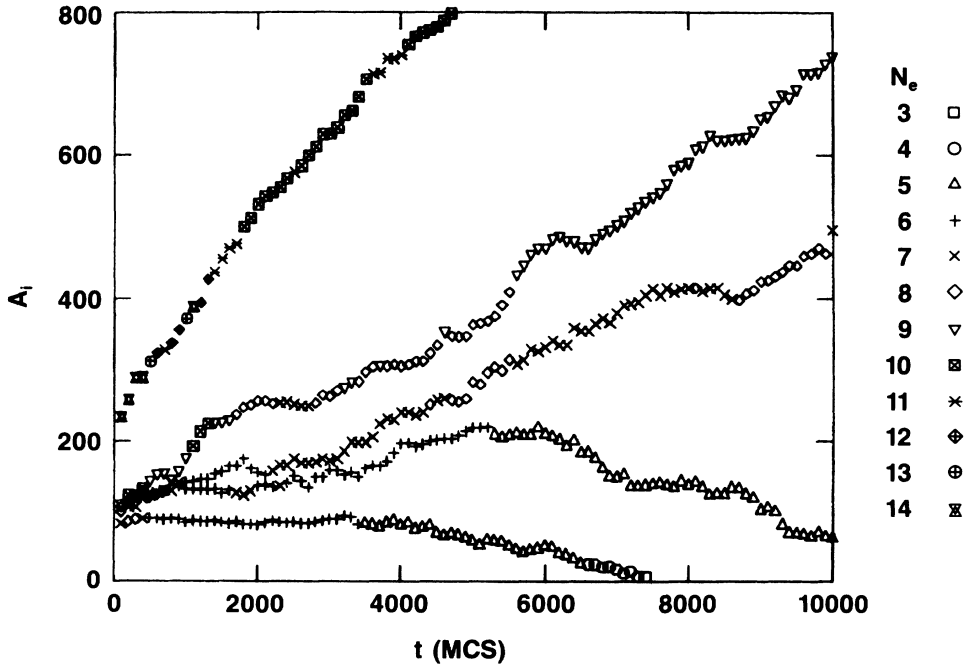

FIG. 9. Time dependence of the area A_i of five randomly chosen grains from the 2D simulations. The symbols represent the number of edges, N_e. As in Fig. 8, the clock was reset to 0 after an initial run of 1000 MCS.

ditional constraint that Eq. (4) be satisfied at all times. They found that the growth kinetics followed Eq. (1) with $n=\frac{1}{2}$ even for very early times. Without this constraint they obtained our previous result, $n=0.41$. To test the local equilibrium property of the growth, we carried out a simulation for the $Q=48$ Potts model in which we followed each grain, monitoring the number of edges as a function of time. This was first done by performing a normal domain-growth simulation in 2D for $Q=48$ on a 200^2 triangle lattice for 1000 MCS until there were 960 grains remaining. In Fig. 8, we present results for the temporal evolution of the area of several individual grains with the same number of edges. Those grains monitored in Fig. 8 were highly unusual in that their number of edges did not change during the majority of the 10000 MCS run. For convenience we have reset the clock to 0 after we started monitoring the number of edges and we have plotted a symbol only when the number of edges equal the number N_e specified in the figure. From Fig. 8, we see that the slope of $\dot{A}_i$ is approximately zero for $N_e=6$ and that the slopes for $N_e=4$ and 8 are approximately of equal magnitude and opposite sign. An average slope for $N_e=5$ and 7 is harder to determine. We must point out that most of the grains change N_e to often to be plotted in this way. Shown in Fig. 9 is the temporal evolution of the area A_i for five more typical grains observed during the 10000 MCS run. A different symbol is used to label the number of edges at a given time. Note how often N_e changes. The data in Fig. 9 are the norm, while those in Fig. 8, are the exceptions.

Thus it appears that for those grains which keep the same number of sides for a long time, Eq. (4) is satisfied. However, there are large fluctuations around the mean slope and for most grains N_e changes too often for Eq. (4) to be applicable. From these results, we may be able to understand why the asymptotic growth regime was hard to obtain in our earlier simulations. Local equilibrium was apparently established very slowly and n appeared to be less than $\frac{1}{2}$. Even though the grains were several hundred sites in size, they were continuously changing their number of edges N_e too rapidly for the system to reach local equilibrium. Every time N_e changes, the microstructure rearranges to accommodate the new growth rate, as per Eq. (4). This accommodation process is not instantaneous but requires a finite amount of time τ. If this time had scaled with the grain size, we would have expected that n would remain less than $\frac{1}{2}$. Apparently, though τ does not scale with the grain size for long times, leading to the observed crossover to $n\approx 0.50$ kinetics for very late times.

[1] I. M. Lifshitz, Zh. Eksp. Teor. Fiz. **42**, 1354 (1962) [Sov. Phys.—JETP **15**, 939 (1962)].

[2] S. A. Safran, Phys. Rev. Lett. **46**, 1581 (1981).

[3] P. S. Sahni, D. J. Srolovitz, G. S. Grest, M. P. Anderson, and S. A. Safran, Phys. Rev. B **28**, 2705 (1983).

[4] M. P. Anderson, D. J. Srolovitz, G. S. Grest, and P. S. Sahni, Acta Metall. **32**, 783 (1984).

[5] D. J. Srolovitz, M. P. Anderson, P. S. Sahni, and G. S. Grest, Acta Metall. **32**, 793 (1984).

[6] K. Kaski, S. Kumar, J. D. Gunton, and P. A. Rikvold, Phys. Rev. B **29**, 4420 (1984).

[7] A. Sadiq and K. Binder, J. Stat. Phys. **35**, 517 (1984).

[8] J. Viñals and J. Gunton, Surf. Sci. **157**, 473 (1985).

[9] K. Kaski, J. Nieminen, and J. D. Gunton, Phys. Rev. B **31**, 2998 (1985); S. Kumar, J. D. Gunton, and K. Kaski, *ibid.* **35**, 8517 (1987).

[10] H. Furukawa, Phys. Rev. A **29**, 2160 (1984).

[11] O. Mouritsen, Phys. Rev. Lett. **56**, 850 (1986); Phys. Rev. B **32**, 1632 (1985).

[12] C. Dasgupta and R. Pandit, Phys. Rev. B **33**, 4752 (1986).

[13] J. Viñals and J. D. Gunton, Phys. Rev. B **33**, 7795 (1986); J. Viñals and M. Grant, *ibid.* **36**, 7036 (1987).

[14] G. S. Grest, M. P. Anderson, and D. J. Srolovitz, in *Computer Simulation of Microstructural Evolution,* edited by D. J. Srolovitz (AIME, Warrendale, Pennsylvania, 1986), p. 21; in *Time Dependent Effects in Disordered Materials,* edited by R. Pynn and T. Riste (Plenum, New York, 1987), p. 365.

[15] J. Wejchert, D. Weaire, and J. P. Kermode, Philos. Mag. B **53**, 15 (1986).

[16] O. Mouritsen, in *Annealing Processes—Recovery, Recrystallization and Grain Growth,* edited by N. Hansen *et al.* (Risø National Laboratory, Roskilde, Denmark, 1986), p. 457.

[17] (a) M. P. Anderson, G. S. Grest, and D. J. Srolovitz, Scr. Metall. **19**, 225 (1985); (b) Philos. Mag. B (to be published). In the first of these two papers and in Ref. 14, we used all the kinetic data ($t\geq 200$ MCS) to determine the growth exponent n in 3D. For this reason the value of n for high Q quoted in these papers, $n=0.39$, is lower than the value $n=0.48$ quoted in the present paper.

[18] For a review for the Ising model, see J. D. Gunton, M. San Miguel, and P. S. Sahni, in *Phase Transitions and Critical Phenomena,* edited by C. Domb and J. L. Lebowitz (Academic, New York, 1983), Vol. 8, p. 267; K. Binder, in *Condensed Matter Research Using Neutrons,* edited by S. W. Lovesey and R. Scherm (Plenum, New York, 1985), p. 1.

[19] S. M. Allen and J. W. Cahn, Acta Metall. **27**, 1085 (1979).

[20] K. Kawasaki, M. C. Yalabik, and J. D. Gunton, Phys. Rev. A **17**, 455 (1978); T. Ohta, D. Jasnow, and K. Kawasaki, Phys. Rev. Lett. **49**, 1223 (1982).

[21] S. A. Safran, P. S. Sahni, and G. S. Grest, Phys. Rev. B **28**, 2693 (1983).

[22] M. Grant and J. D. Gunton, Phys. Rev. B **28**, 5496 (1983).

[23] G. F. Mazenko and O. T. Valls, Phys. Rev. B **27**, 6811 (1983); G. F. Mazenko, O. T. Valls, and F. C. Zhang, *ibid.* **31**, 1579 (1985).

[24] M. K. Phani, J. L. Lebowitz, M. H. Kalos, and O. Penrose, Phys. Rev. Lett. **45**, 366 (1980); P. S. Sahni *et al.*, Phys. Rev. B **24**, 410 (1981).

[25] E. T. Gawlinski, M. Grant, J. D. Gunton, and K. Kaski, Phys. Rev. B **31**, 281 (1985).

[26] J. Viñals, M. Grant, M. San Miguel, J. D. Gunton, and E. T. Gawlinski, Phys. Rev. Lett. **54**, 1264 (1985).

[27] G. Mazenko, O. Valls, and F. C. Zhang, Phys. Rev. B **31**, 4453 (1985); **32**, 5807 (1985).

[28] D. Huse, Phys. Rev. B **34**, 7845 (1986).

[29] A. B. Bortz, M. H. Kalos, and J. L. Lebowitz, J. Comput.

Phys. **17**, 10 (1975).
[30]Z. W. Lai, G. F. Mazenko, and O. T. Valls, Phys. Rev. **37**, 9481 (1988).
[31]A. Milchev, K. Binder, and D. W. Heermann, Z. Phys. B **63**, 521 (1986).
[32]S. K. Kurtz and F. M. A. Carpay, J. Appl. Phys. **51**, 5725 (1980).
[33]N. P. Louat, Acta. Metall. **22**, 721 (1974).
[34]C. W. J. Beenakker, Phys. Rev. A **37**, 1697 (1988).
[35]W. W. Mullins, J. Appl. Phys. **59**, 1341 (1986); W. W. Mullins and J. Viñals (unpublished).
[36]J. von Neumann, in *Metal Interfaces* edited by C. Herring (ASM, Metals Park, Ohio, 1952), p. 108.
[37]W. W. Mullins, J. Appl. Phys. **27**, 900 (1956).